

## Composition and morphology of tungsten limiter surface after interaction with deuterium plasma in Globus-M tokamak

A.N. Novokhatsky<sup>1</sup>, V.K. Gusev<sup>1</sup>, A.E. Gorodetsky<sup>2</sup>, R. Kh. Zalavutdinov<sup>2</sup>, A.P. Zakharov<sup>2</sup>,  
N.V. Litunovsky<sup>3</sup>, A.V. Markin<sup>2</sup>, I.V. Mazul<sup>3</sup>, N.V. Sakharov<sup>1</sup>, A.V. Voronin<sup>1</sup>

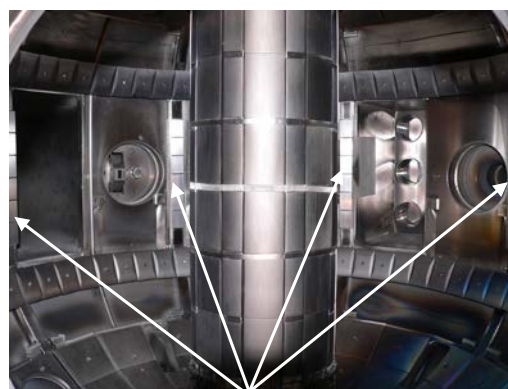
<sup>1</sup> *A.F.Ioffe Physical-Technical Institute, Russian Academy of Sciences, St. Petersburg, Russia*

<sup>2</sup> *A.N.Frumkin Institute of Physical Chemistry and Electrochemistry, Russian Academy of Sciences, Moscow, Russia*

<sup>3</sup> *D.V.Efremov Institute, St. Petersburg, Russia*

The main concerns of application of graphite as plasma-facing material are associated with its strong chemical affinity to hydrogen, which leads to chemical erosion and formation of hydrogen-rich carbon layers. These layers can store a significant fraction of the total tritium fuel that prevents the use of carbon materials in ITER. Tungsten is the top candidate for the plasma-facing material in ITER due to its capability to survive in high-temperature and high neutron irradiation environment [1].

To study an interaction of tungsten with intensity deuterium plasma the tungsten poloidal limiters were installed on an outer cylindrical part of the Globus-M vacuum vessel in 2004 (Fig. 1). The



**Tungsten limiters**

*Fig. 1. Tungsten limiters in Globus-M tokamak*

The tungsten limiters were made from 2.7 mm thick tungsten tiles brazed onto copper substrates. The VMP tungsten ('tungsten of powder metallurgy') produced by Polema JSC, Russia completely satisfies the ITER's quality specification for this material and supposed to be used for armoring of the ITER Divertor Dome [2]. The tungsten poloidal limiters have been removed and exchanged by graphite tiles placed on the outer cylindrical part of the vacuum vessel in 2007. In February, 2008 for RF-heating experiments the protection tiles configuration was changed. To increase a vacuum wall reflection coefficient required for RF-heating experiments the protection graphite tiles placed on the outer cylindrical part of the vacuum vessel were removed and exchanged by eight discrete tungsten poloidal limiters. In 2011, after 13770 pulses (total duration ~ 1400 s), the limiters were taken for postmortem analysis. The tungsten tiles were manufactured by means of Electrical Discharge Machining (EDM) cut-out from 3 mm thick VMP tungsten plate and then grinded from both sides down to the thickness of 2.7 mm. Finally, also by grinding, four 1mm × 45° facets were formed on edges

of tile surface faced to plasma. Substrates for brazing of the tungsten tiles were manufactured from 2 mm copper sheets. All substrates have two 20×20 mm brazing contact areas for two tungsten tiles. Limiting of brazing area was necessary for reducing of thermomechanical stresses in the brazed joint that is caused by a considerable difference of thermal expansion coefficients of two brazed materials. Also, to avoid forming of stress-concentrating zero angles in the perimeter of local joint between W and Cu surfaces, the contact areas of the substrates were made uplifted for 0.3 mm with respect to rest surface. Besides, these contact ‘islands’ were supplied with side-edge grooves for draining of the excess filler (Fig. 2).

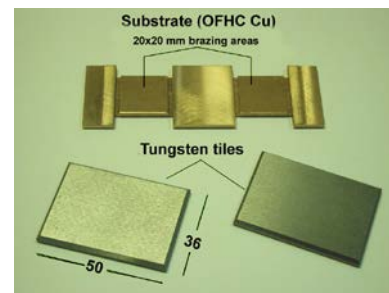


Fig. 2. Details of tungsten limiters

The copper based alloy STEMET 1108M ( $\text{Cu}_{\text{base}}\text{InNiSnMn}$ ) filler alloy in a form of 50  $\mu\text{m}$  thick and 20 mm ribbon was chosen for brazing of the tiles to the substrates. Prior to brazing, for better adhesion with the filler, joint area on the rear side of all tungsten tiles was electrochemically coated with 4-7  $\mu\text{m}$  layer of nickel. Straight before brazing the tungsten tiles were washed in an ultrasonic bath; the substrates and filler – deoxidized, washed in run water and properly dried. Vacuum brazing of the limiters was performed in electron beam facility TSEFEY-M [3]. Heating of the limiters up to brazing temperature of 1083 K has been realized by raster-scanning electron beam with a rate of about 2 K/s. Dynamics of temperature controlled with a help of two thermocouples installed in edge holes in the substrates. After 3 minutes of soak at maximal temperature the beam was switched off and then the limiter element cooled free down to 300 K. Vacuum through all brazing procedure was supported in a level of  $\sim 2 \times 10^{-5}$  Torr.

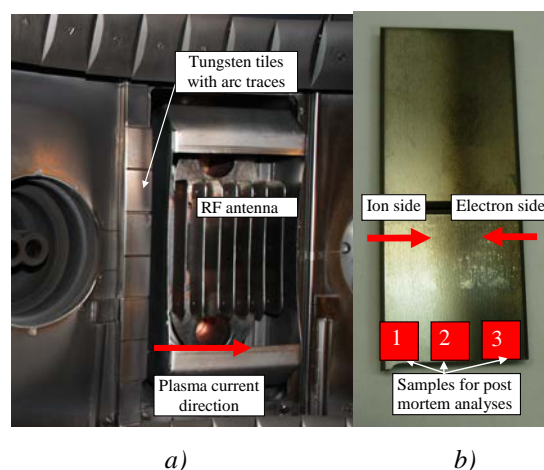


Fig. 3. a) Tungsten limiter with arc traces  
b) Samples for postmortem analyses

For postmortem analysis a limiter tungsten plate located nearby an RF antenna was chosen (Fig. 3a). The limiter was investigated because a part of the tungsten plate surface was covered by films. This part of the plate was situated in the shadow of the RF antenna. Three samples (No 1, 2 and 3) were cut mechanically from the plate (Fig. 3b).

Chemical composition of the samples was studied by electron probe microanalysis (EPMA) on

a microanalyzer Camebax (Cameca, France) equipped with a Si(Li) energy dispersive spectrometer. Characteristic X-rays were generated by electron beam bombardment at 15 kV and

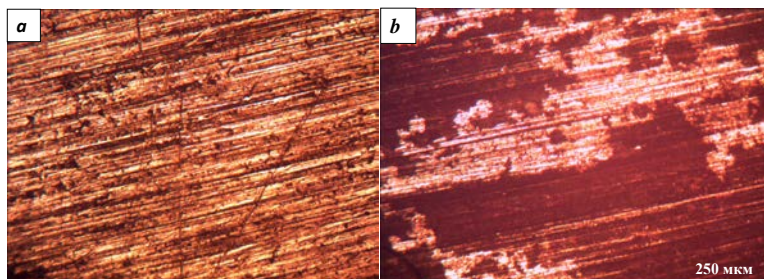
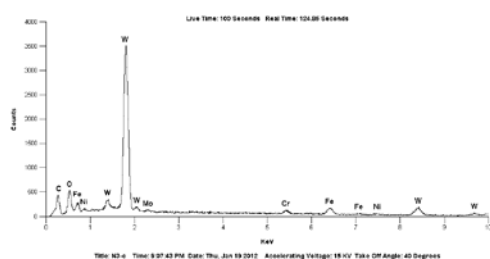


Fig. 4. Optical micrographs of the samples No 1 (a) and 3 (b)

150 nA under residual vacuum of  $10^{-6}$  Torr. The beam raster and the take-off angle (with respect to the sample surface) of the emitted X-rays were  $50 \times 50 \mu\text{m}^2$  and  $40^\circ$ , respectively. Analysis time was 100 s.



Element	C	O	Cr	Fe	Ni
Areal density, $\mu\text{g}/\text{cm}^2$	24.40	26.25	14.55	35.41	15.44
At. %	41.90	33.83	5.77	13.08	5.42

Fig. 5. EPMA spectrum of the sample No 3

areal densities of chemical elements in the near-surface layers were calculated by a code based on the Yakowitz–Newbury method [4]. Bulk diamond,  $\text{SiO}_2$ , Cr, Fe, and Ni were used as standards for the analysis of C, O, Cr, Fe, and Ni. Optical micrographs of the samples No 1 and 3 are shown in Fig. 4. On the left micrograph one can see practically clean tungsten surface but on the right micrograph there are black and light areas. From EPMA data it follows that the black

areas of the surface of the sample No 3, that was situated in the shadow of the RF antenna, were covered with films containing carbon, oxygen and main elements of stainless steel (Fig. 5). Structure of the tungsten samples (No 1, 2 and 3) was investigated by means of X-ray diffraction (XRD). The XRD analysis was fulfilled using a diffractometer DRON-3 with a copper tube ( $\lambda_{\text{Cu}} = 0.154 \text{ nm}$ ) and a graphite monochromator. The registration of diffracting beams was carried out in the range of angles  $2\theta$  from 5 to  $90^\circ$  with step  $0.05^\circ$  and exposition time in each point 3 s (for tungsten a depth of analysis  $\sim 1 \mu\text{m}$  [5]).

areal densities of chemical elements in the near-surface layers were calculated by a code based on the Yakowitz–Newbury method [4]. Bulk diamond,  $\text{SiO}_2$ , Cr, Fe, and Ni were used as standards for the analysis of C, O, Cr, Fe, and Ni. Optical micrographs of the samples No 1 and 3 are shown in Fig. 4. On the left micrograph one can see practically clean tungsten surface but on the right micrograph there are black and light areas. From EPMA data it follows that the black

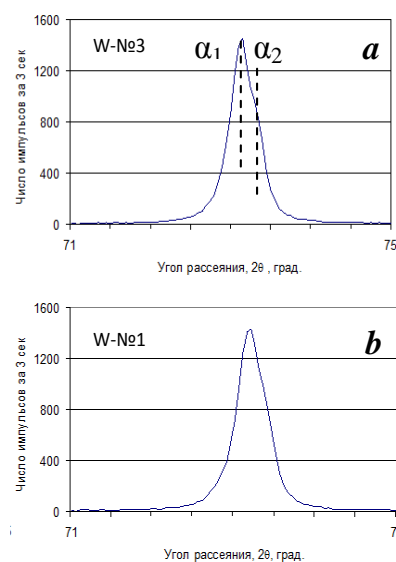


Fig. 6. Splitting of W(211) reflection (scattering angle  $2\theta = 73.2^\circ$ ) on  $\alpha_1$  and  $\alpha_2$  duplets (a) and (b) depending on a degree of imperfection (No 3 and 1)

Metallic tungsten with body-centered lattice (lattice parameter  $a = 0.317$  nm) was observed on all XRD spectra of the samples. However there were some weak peaks connected with graphite, iron and nickel on the XRD spectrum of the sample No 3. Minimal imperfection was registered for the sample No 3 because a splitting of W(211) reflection took place (Fig. 6a) as opposed to W(211) reflection for the sample No 1 (Fig. 6b). This fact is confirmed by comparison of ratios of W(220) peak intensities to W(110) peak intensities (maximal intensity) for each sample: No 1 - 6.8%, No 2 - 7.0%, No 3 - 7.6%. Lowering of W(220) peak intensity is connected with accumulation of various deformation defects in the analyzed layer. Probably, this is caused by plasma flow, which was directed to the samples No 1 and 2, where the sample No 3 was situated in the shadow of the RF antenna.

Deuterium retention was evaluated by degassing the samples No 1 and 3 in a Thermal Desorption Spectroscopy (TDS) setup. The samples were placed inside a quartz tube which was heated by an outer heater. The temperature was measured with Pt-Rh thermocouple, welded to the samples through a nickel intermediate plate. The released molecules HD, D<sub>2</sub> and some others were detected by a quadrupole mass spectrometer (Extorr XT200M). The quadrupole was calibrated by pumping a definite amount of the gas (H<sub>2</sub> or D<sub>2</sub>).

Degassing curves of HD and D<sub>2</sub> molecules from the samples No 1 and 3 are shown in Fig.7. Integrating the curves gives a total deuterium retention of  $3 \times 10^{20}$  D/m<sup>2</sup> in sample No 1 and  $1.5 \times 10^{21}$  D/m<sup>2</sup> in sample No 3. It should be noted that the samples exhibit similar degassing behavior. One explanation for higher retention in sample No 3 is that deuterium is codeposited with carbon to form D-rich layers. On the other hand the redeposited layers on the sample No 3 might change the surface recombination coefficient that also gives rise the D retention.

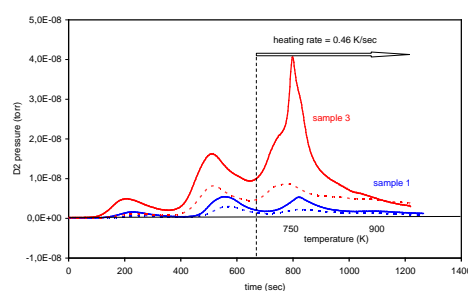


Figure 7. Desorption spectra of D<sub>2</sub> (solid) and HD (dash) from samples No 1 and 3. Above 700 K the heating rate is 0.46 K/sec

The work is supported by the IAEA Research Contracts No: 16939, RFBR grant 11-08-00813-a, RF Ministry of Education and Science contracts; No. 16.518.11.7003; No. 16.552.11.7002, No. 11.G34.31.0041.

## References

- [1] R. Neu, Plasma Phys. Control. Fusion 53 (2011) 124040 (24 p).
- [2] V. Barabash et al. J. of Nuclear Materials 307-311 (2002) 1524.
- [3] V.K. Gagen-Torn et al. Proc. of 18<sup>th</sup> Symposium on Fusion Technology, Karlsruhe, August 1994, p. 363.
- [4] J. Goldstein et al. Scanning Electron Microscopy and X-ray Microanalysis, 1981 (New York: Plenum) 651 p.
- [5] R.W. James The Optical Principles of the Diffraction of X-rays. London. Bell. 1950. 570 p.